

The Effect of High-intensity Focused Ultrasound on Intracanal Bacterial Reduction, Chemical Structure, and Mechanical Properties of Root Dentine

 Sheetal Maria RAJAN,¹  Barsha SHRESTHA,¹  Mostafa M. A. ELKHOLY,¹
 Hany Mohamed Aly AHMED,²  Amr FAWZY¹

¹UWA Dental School, The University of Western Australia, Nedlands, Australia

²Department of Restorative Dentistry, University of Malaya, Faculty of Dentistry, Kuala Lumpur, Malaysia

ABSTRACT

Objective: High-intensity focused ultrasound (HIFU) has demonstrated significant efficacy in eradicating bacteria from substrates emerging as a promising solution for root canal disinfection. This *in-vitro* study investigated the effects of HIFU on reducing intracanal bacteria and its impact on the chemical and mechanical properties of root dentine. It also aimed to demonstrate acoustic wave penetration and distribution within the root canal system (RCS) and characterize the associated temperature changes.

Methods: Eighty-two extracted premolar teeth with single canals, infected with *Enterococcus faecalis* (*E. faecalis*) and cultured for two weeks, were randomly assigned to four groups: negative control, 4% sodium hypochlorite (NaOCl), 60 s HIFU, and 120 s HIFU (operated at 250 kHz/20W). Post-treatment, biofilm samples were collected from the root canals to assess viable bacterial cells using colony-forming unit (CFU) and 3-[4,5-dimethylthiazol-2-yl]-2,5 diphenyl tetrazolium bromide (MTT) assays. The root canal surfaces were subsequently examined using scanning electron microscopy, confocal laser scanning microscopy (CLSM), microhardness, and Raman spectroscopy. Acoustic wave penetration, distribution, and temperature changes within the RCS were examined using CLSM and thermal camera.

Results: HIFU at 60 s and 120 s consistently demonstrated superior anti-bacterial efficacy against *E. faecalis* biofilms compared to 4% NaOCl. MTT and CFU assays revealed a significant reduction in biofilm viability, particularly at 120 s of HIFU exposure ($p < 0.05$). CLSM and SEM analyses demonstrated enhanced penetration and detachment of biofilms, as well as improved smear layer removal and preservation of dentinal tubules, especially at 120 s of HIFU exposure. HIFU treatment did not adversely affect the amide/mineral content of root dentine or its surface microhardness. Additionally, HIFU enhanced acoustic wave propagation and resulted in a controlled increase in temperature within the root canal over time.

Conclusion: This minimally invasive approach shows promise for removing bacterial biofilms in the RCS, positioning HIFU as a valuable adjunctive treatment for enhancing root canal disinfection.

Keywords: Acoustic wave, bacterial reduction, *Enterococcus faecalis*, high-intensity focused ultrasound (HIFU), root dentine, sodium hypochlorite

Please cite this article as:

Rajan SM, Shrestha B, Elkholy MMA, Ahmed HMA, Fawzy A. The Effect of High-intensity Focused Ultrasound on Intracanal Bacterial Reduction, Chemical Structure, and Mechanical Properties of Root Dentine. *Eur Endod J* 2025; 10: 116-126

Address for correspondence:

Amr Fawzy
UWA Dental School, The University of Western Australia, Nedlands, Australia
E-mail: amr.fawzy@uwa.edu.au

Received : August 13, 2024,

Revised : October 02, 2024,

Accepted : November 13, 2024

Published online: March 18, 2025

DOI 10.14744/eej.2024.77487

This work is licensed under a Creative Commons

Attribution-NonCommercial 4.0 International License.



HIGHLIGHTS

- HIFU's acoustic waves and heat formed disrupt bacterial cell walls.
- HIFU, especially for 120s, efficiently eliminates *E. faecalis* biofilms.
- HIFU treatment exhibits better biofilm penetration and detachment than NaOCl.
- HIFU maintains dentine structure and mineral content without altering its integrity.

INTRODUCTION

Intra-radicular bacterial infection is recognized as the primary cause of both primary and post-treatment apical periodontitis, highlighting the critical importance of complete root canal disinfection for the success of both initial treatment and retreatment procedures (1, 2). Although attaining complete bacterial eradication remains an ultimate goal, its clinical realization is considerably challenging owing to bacterial persistence within the root canal system (RCS). This persistence is evidenced by residual biofilms on unprepared dentinal walls and irregularities (3, 4) in the main canal lumen, bacterial invasion of the dentinal tubule (5), and microbial resistance to disinfecting irrigants and medicaments (6, 7).

These challenges prompted the consideration of adjunct disinfection protocols aimed at enhancing the efficacy of irrigants. These protocols range from simple agitation to more sophisticated approaches such as photodynamic therapy and the Photon-Induced Photoacoustic Streaming technique (6, 8, 9). These interventions aim to achieve maximal reduction of residual intracanal bacteria. Sodium hypochlorite (NaOCl) remains the gold standard for disinfection, but its efficacy is contingent on factors such as concentration, volume, and exposure time (10). While longer exposure times improve bacterial reduction, excessive exposure can lead to the dissolution of the organic dentine matrix and structural damage to the root (11, 12). Additionally, even with extended exposure, NaOCl struggles to penetrate complex anatomical regions such as lateral canals and apical deltas, highlighting the need for careful control of its application (13–15).

The evolution of high-intensity focused ultrasound (HIFU) for disrupting bacterial biofilms from a substrate with minimal surface damage, achieved through the generation of cavitation bubbles, represents an advancing field in dental research (16–18). The primary effect of HIFU arises from inertial cavitation, a phenomenon occurring at high intensities that involves the vigorous acceleration and collapse of oscillating bubbles. This process results in elevated fluid shear rates at the bacterial cell membrane (17). The concentrated energy released during the collapse of cavitation bubbles can have significant consequences for bacterial cell integrity. This includes mechanical damage due to pressure and pressure gradients, shear forces generated by microstreaming, chemical attacks arising from the formation of free radicals, and the production of bactericidal hydrogen peroxide (19–21). Moreover, HIFU has the capability to remove the smear layer, reveal the dentinal tubules, and produce a textured dentine surface with increased exposure time (22). All these effects, however, are dependent on the targeted tissue and the HIFU operation parameters. Despite advancements in root canal disinfection, complete bacterial eradication remains elusive due to microbial persistence within the dentinal tubules and resistance to conventional irrigants. While HIFU presents a promising non-invasive alternative for biofilm disruption, its efficacy in achieving deep dentinal penetration and its potential effects on root dentine integrity require further investigation to optimize its clinical applicability.

This *in-vitro* study aimed to investigate the effect of HIFU on intracanal bacterial reduction and its effect on inducing

chemical and/or mechanical changes in root dentine. In addition, it aimed to demonstrate acoustic wave penetration and distribution within RCS and to characterize the associated temperature changes.

MATERIALS AND METHODS

Sample Size Calculation

The sample size was determined utilizing G*Power 3.1.9.7 (HHU, Düsseldorf, Germany) based on the specified parameters: for ANOVA with one-way analysis, using an effect size of $f=0.4$, α err prob=0.05, and power=0.8 (23, 24). Consequently, the minimum required sample size for the study was 76 samples.

Tooth Selection

Ethical approval from the institutional review boards (University of Western Australia Human Research Ethics Committee grant #RE 2019/RA/4/20/5863) was obtained, and the study was conducted in accordance with the Declaration of Helsinki. Eighty-two human single-rooted mandibular premolars with single-root canals were included in this study. Teeth with incomplete root formation, root caries, root fractures, or external root resorption were excluded. Preoperative 2D radiographic images were taken to confirm that the teeth had a single canal with no internal root resorption or previous root canal treatment. Following this, the teeth were disinfected in a 0.5% chloramine-T solution for 24 h and stored in a 0.1% thymol solution, then refrigerated at 4°C until use. Before experimentation, the teeth were autoclaved for 15 min at 121°C.

The teeth were decoronated with a diamond blade (0.3 mm thickness) using a slow-speed diamond saw (IsoMet, Buehler, Düsseldorf, Germany) under water cooling, and the root lengths were adjusted to a standardized length of 12 mm. The root canals were instrumented to 1 mm short of the root apex up to stainless-steel K-files size #40 (Maillefer Instruments SA, Ballaigues, Switzerland) while irrigating with 1% NaOCl (DentaLife, Victoria, Australia). Further, the root canals were flushed with a sterile saline solution, followed by irrigation with a 17% EDTA solution for 1 min to eliminate the smear layer. Subsequently, the specimens were thoroughly washed with distilled water in an ultrasonic bath, to have less deleterious effects on dentine microstructure and remove the canal wall smear layer (17).

E. Faecalis Growth and Root Canal Inoculation

The bacteria were cultured according to a previously described protocol (16, 17). *E. faecalis* (NCTC 8213) was grown overnight in Brain-heart Infusion (BHI) broth (Sigma-Aldrich, Australia) at 37°C and subsequently adjusted to 10⁸ CFU/mL concentration. Each root canal specimen was individually positioned upright in sterile 48-well plates containing 400 µL of BHI media. Subsequently, 100 µL of the prepared bacterial suspension was added to each well and allowed to grow for two weeks under aerobic conditions at 37°C and 100 rpm to facilitate biofilm formation. To provide nutrients, the growth medium was replenished every 48 h. Following a two-week incubation, *E. faecalis* biofilm development was confirmed by scanning electron microscopy (SEM) on randomly selected specimens, ensuring biofilm formation at all levels of the root canals prior to treatment (25).

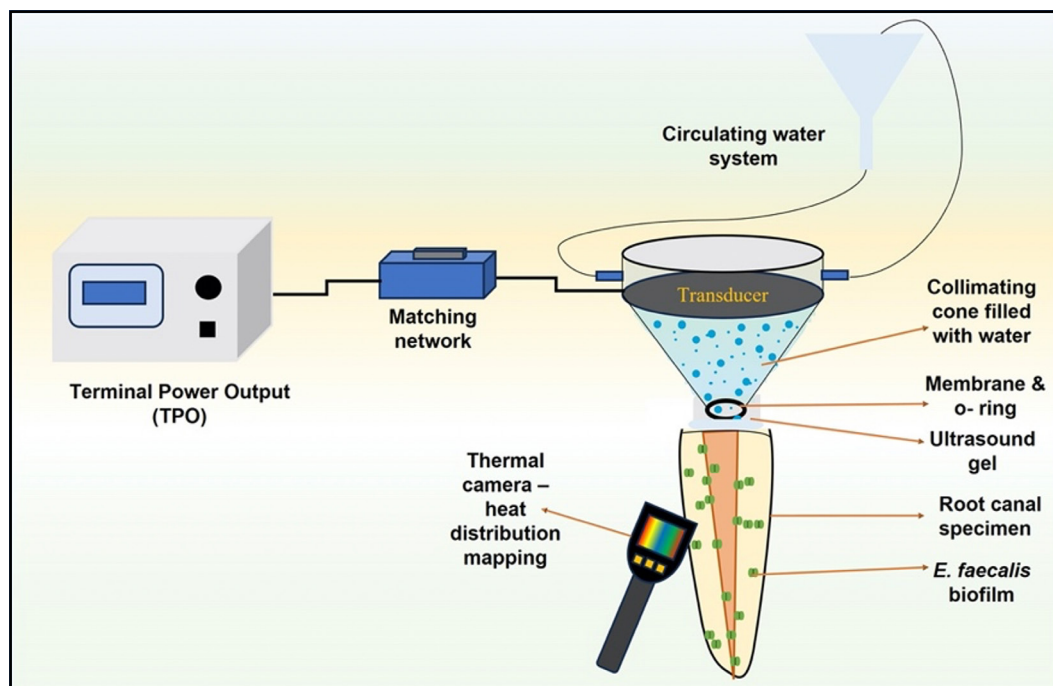


Figure 1. The schematic illustration depicts the experimental setup of HIFU for intracanal bacterial reduction in root canal dentine (250 kHz, 20W). The HIFU setup includes a terminal power output (TPO), a 50 Ω matching network, and a focused ultrasound transducer operating at 250 kHz. The transducer features a collimating cone filled with degassed water, connected to a circulating water system via syringe connections. The opening of the cone is sealed with a polyurethane membrane, secured with an O-ring around the transducer's edge. A thermal camera, positioned perpendicular to the root canal specimen interface, was used to measure the heat distribution during HIFU exposure

HIFU: High-intensity focused ultrasound

Samples Grouping

Out of 82 samples, a total of 76 teeth were randomly allocated into four groups (n=19 each) using computer-generated randomization in Excel (Microsoft, Redmond, WA, USA). The remaining 6 teeth were used for the HIFU penetration/distribution and temperature change experiments. The four groups were defined as follows: the Negative control group (NC) with no intervention, the Positive control group (PC) which underwent irrigation with 4% NaOCl (26, 27) using conventional needle irrigation with double side-vented needles (Henry Schein, Australia) for 1 min at a flow rate of 0.2 mL/s (28), and two experimental groups exposed to HIFU for 60 s and 120 s.

HIFU Experimental Setup and Root Canal Exposure

Figure 1 shows the HIFU experimental setup. In brief, a 64 mm bowl-shaped piezoelectric ceramic transducer with a resonance frequency of 250 kHz (H-115, Sonic Concepts Inc, WA, USA) equipped with a transparent polycarbonate collimating cone, with a height of 50 mm and diameter of 3.1 mm was used in the study. The transducer has a geometrical focus of 63.2 mm, and a focal depth of 51.74 mm, respectively. A custom-made electrical matching network was connected between the Terminal Power Output (TPO) (Sonic Concepts Inc, WA, USA) and the transducer. The collimating cone was filled with degassed water using syringe connections, and the opening was covered with a polyurethane membrane, fixed around the edges of the transducer using an O-ring to secure the seal. The geometry of the cone enabled the center of the focal spot to be on the membrane.

Following the two-week incubation of the root canal specimens, BHI media was removed, and the specimens were gently rinsed with sterile phosphate-buffered saline (PBS). Subsequently, 100 μ L of ultrasound coupling gel (sterile) was applied to the surface of the specimens before exposing them to varying HIFU exposure. The HIFU device was operated at an output power of 20 W in continuous mode, achieving a peak focal pressure of 1.12 MPa_{Pk} for two different exposure times: 60 s, and 120 s (HIFU parameters were determined based on our preliminary investigations).

Microbiological Evaluation

MTT and colony forming unit (CFU) assay

After treatment, the metabolic activity of *E. faecalis* biofilms was evaluated using a 3-[4,5-dimethylthiazol-2-yl]-2,5 diphenyl tetrazolium bromide (MTT) assay kit (0.5 mg/mL MTT solution) (Sigma-Aldrich, Australia), following the manufacturer's guidelines. To release the bacteria remaining attached, the treated root canals (n=7) were subjected to ultrasonication for 10 min in vials containing 500 μ L of distilled water. The bacterial suspension was then aliquoted in triplicates into a 96-well plate, with each well receiving 100 μ L of the suspension. Then, 10 μ L of MTT reagent was added to each well, and the plate was covered and incubated at 37°C for 4 h. Following incubation, the reagent was aspirated, and 100 μ L of the solubilizing solution was added, and subjected to incubation overnight at 37°C (17). Absorbance at 600 nm, with a reference wavelength of 700 nm, was measured using a spectrophotometer (SunriseTM, Tecan, Switzerland).

To further confirm the viability of the bacteria after treatment, a CFU assay was conducted as outlined in previous methods (16). In brief, treated root samples (n=7) were placed in vials containing 500 µL of sterile distilled water and subjected to ultrasonication for 10 mins to detach the adhered bacteria. Upon ultrasonication, 100 µL of the solution was serially diluted, plated on BHI agar plates, and incubated for 24 h at 37°C. The number of viable colonies was determined using the following formula (17):

$$\text{CFU/mL} = \frac{\text{Number of colonies} \times \text{Total dilution factor}}{\text{Volume of culture plated (mL)}}$$

Confocal laser scanning microscopy (CLSM)

After treatment, the root canal specimens (n=3 per group) were stained for 10 mins with LIVE/DEAD™ BacLight™ Bacterial Viability Kit (ThermoFisher Scientific, MA, USA) containing the dyes Propidium iodide (PI) and Syto9 following manufacturer's guidelines. The samples were washed with 500 µL of PBS, followed by fixation for 10 mins using 4% paraformaldehyde solution. Post-fixation, the root canal specimens were split longitudinally using a mallet and chisel. The split quadrants (n=12 per group) were visualized using Nikon Ai Si Confocal Microscopy (Nikon Instruments Inc, NY, USA). The excitation wavelength for Syto9 and PI was centered at ~485 nm, whereas the fluorescence intensity was measured at ~530 nm (green) and ~630 nm (red), respectively. Three different locations (coronal, middle, and apical) on each specimen were scanned layer-by-layer (z-stack) and combined to get a representative image.

Scanning Electron Microscopy (SEM)

Post-treatment the root canal specimens from each group were longitudinally split by employing a mallet and chisel into two halves (n=3 per group; total after splitting (n=6 per group)). The specimens were then dehydrated through a sequence of increasing ethanol concentrations using a PELCO BioWave microwave at 250 W (Ted Pella, Inc., USA). After dehydration, the samples were mounted on aluminium stubs with copper tape and coated with platinum (~3 mm) using a Polaron SC7640 sputter coater (Quorum Technologies Ltd, U.K). Representative SEM images of each root canal were captured at 7500x magnification using Zeiss 1555 VP-FESEM (Carl Zeiss, Oberkochen, Germany) operated at an accelerating voltage of 10 kV.

SEM images of the apical regions of the root canal were used to semi-quantitatively assess the smear layer coverage on root canal walls across the treatment groups. Five specialists independently examined and calibrated the images in a single-blind manner using a scoring system developed by Gutmann et al. (29). The scoring criteria were as follows:

Score 1: minimal or no smear layer, covering less than 25% of the specimen; with dentinal tubules patent and clearly visible. Score 2: mild to moderate or patchy smear layer, covering 25-50% of the specimen; with many dentinal tubules patent and visible. Score 3: moderate amounts of dispersed or aggregated smear layer, covering 50-75% of the specimen; with minimal or no patency or visibility of dentinal tubules. Score 4: heavy smear layer, covering over 75% of the specimen; with no patent or visible dentinal tubules.

Raman Analysis of the Root Canal Dentine

A Raman microscope (WITec alpha 300RA; Germany) equipped with a laser that emitted light at an excitation wavelength of 765 nm was used to analyze and determine the chemical composition of the root canal surface after exposure to varying HIFU parameters. The Raman microscope was configured to perform a full scan across the range of 300-1800 cm⁻¹. Treated root canal specimens were split longitudinally into two halves (n=6 per group; total after splitting n=12 per group) and mounted on a glass slide. Multiple random sites were then examined using a 20× objective lens. Spectra were collected with an integration time of 1 s and 40 accumulations, employing 600 lines/mm grating. The mineral and organic bands present on the surface of the root canal dentine within each specimen were investigated.

Vickers Microhardness Testing of the Root Canal Dentine

The surface microhardness of the treated root canal specimens split longitudinally into two halves (n=6 per group; total after splitting n=12 per group) was measured using a Microhardness tester (Duramin-40; Struers, Australia). The measurements were taken at two specific locations: 500 µm and 1000 µm from the pulp-dentine interface (30). During each measurement, 5 indentations were made on the surface. A force of 100 g was applied perpendicularly to the indentation surface for a dwell time of 10 s. The reported result represents the average value obtained from these indentations for each specimen.

HIFU Penetration/Distribution and Temperature Change within RCS

Prepared and sterilized teeth (n=8 with a total of four surfaces per group) without bacterial inoculation were used to visualize the penetration/distribution pattern of HIFU and associated temperature changes within the RCS. The root canal specimens were injected with ultrasound gel containing Fluorescein isothiocyanate (FITC) dye and subjected to the same HIFU setup with varying times of 60 s and 120 s. Each specimen was then split longitudinally into quadrants and was visualized using Nikon Ai Si Confocal Microscopy (Nikon Instruments Inc, NY, USA) to evaluate the penetration distance attained with HIFU exposure. Concurrently, temperature variations in the root canal specimens during the experiment were monitored and recorded using an infrared thermal imaging camera (Opatrix PIX), and its dedicated software packages (Opatrix PIX Connect) (31, 32). The camera was positioned perpendicularly to the specimen and captured continuous thermal images throughout the treatment. The resulting images were analyzed to evaluate temperature fluctuations, which were consistent with those observed during the course of the experiments, and the average values were calculated to ensure reliable data interpretation.

Statistical Analysis

Statistical analysis was conducted utilizing SPSS Statistics (version 23.0, Armonk, USA). The Shapiro-Wilk test (p>0.05) was employed to assess the normality of data distribution, while Levene's test (p>0.05) confirmed the homogeneity of variance. Given that the data followed a normal distribution, results were expressed as mean ± standard deviation and analyzed using one-way ANOVA followed by Tukey's post-hoc test. For determining statistical significance, the threshold was set at 0.05 (p<0.05).

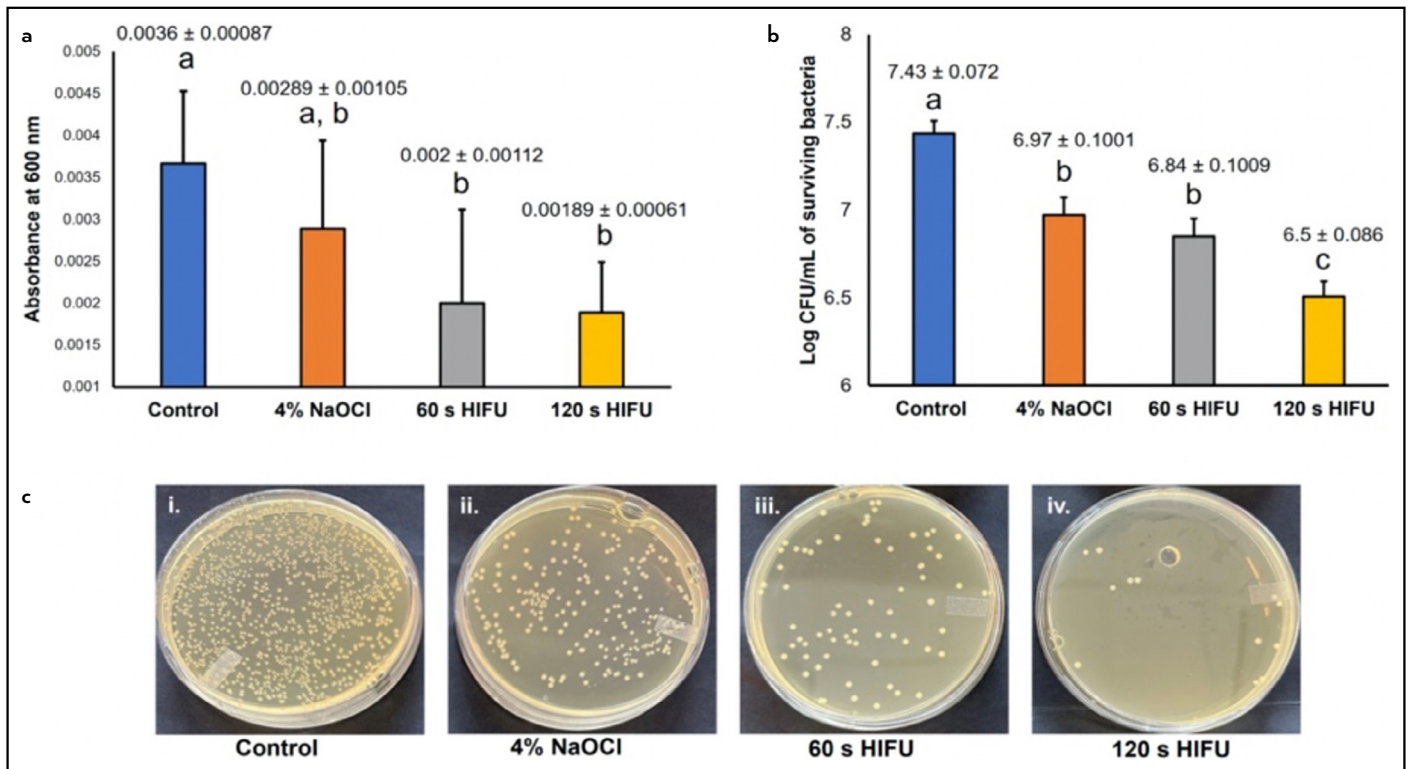


Figure 2. Bar charts of (a) MTT assay measuring the % of bacterial viability among the treated groups. (b) Log number of bacteria (CFUs) in an mL after different treatments. Data are presented as the mean ± standard deviation. Significant differences (dissimilar letters indicate significant difference) between control and treatment groups ($p < 0.05$). (c) CFU plates, which serve as visual representations of the antibacterial effectiveness exhibited by the treatment groups

NaOCl: Sodium hypochlorite, HIFU: High-intensity focused ultrasound, MTT: 3-[4,5-dimethylthiazol-2-yl]-2,5 diphenyl tetrazolium bromide, CFU: Colony-forming unit

RESULTS

MTT and Colony-forming Units Assay

The metabolic activity of *E. faecalis* biofilm across all experimental groups is illustrated in Figure 2a. Notably, there was a significant decrease in the relative metabolic activity observed in the HIFU treatment groups when compared to the control group ($p < 0.001$). To further confirm the anti-bacterial effects among the treatment groups, a CFU assay, expressed as \log_{10} CFU/mL, was conducted (Fig. 2b). The analysis of variance showed a noteworthy reduction in CFU/mL when comparing the control group to 120 s of HIFU ($p < 0.05$). Furthermore, the Tukey test indicated that the \log_{10} CFU/mL of remaining bacteria was significantly higher in the 4% NaOCl and 60 s HIFU group, in comparison to 120 s of HIFU ($p < 0.05$).

Confocal Laser Scanning Microscopy (CLSM)

Representative images illustrating the penetration of *E. faecalis* biofilms into the dentinal tubules of the coronal, middle, and apical parts of the root canal are depicted in Figure 3a. In the fluorescent image of the control group, (Fig. 3a (i-iii)) all the bacteria emitted green fluorescence, indicating that they were viable, with no signs of red fluorescence (signifies dead/damaged bacteria) within the dentinal tubules. Conversely, the extent of red fluorescence within the dentinal tubules varied in the 4% NaOCl and HIFU treatment groups. Treatment with 4% NaOCl (Fig. 3a (iv-vi)) for 1 min was significantly less effective in eliminating bacteria present in the coronal, mid-

dle, and apical regions when compared to the HIFU-treated groups. Exposure to HIFU for 120 s (Fig. 3a (x-xii)) caused a shift from predominantly green bacterial fluorescence to red, signifying the most substantial bacterial inhibition, and was able to penetrate deep within the dentinal tubules.

Scanning Electron Microscopy (SEM)

The SEM images of the control group revealed that *E. faecalis* formed a complex biofilm structure, surrounding the bacteria within a dense and heavy matrix. These structures firmly attach to the root canal wall, concealing the dentine surface with the dentinal tubules being mostly indiscernible (Fig. 3b (i-iii)). When treated with 4% NaOCl, there was a noticeable disruption of the biofilm interconnections, but it remained attached to the root surface (Fig. 3b (iv-vi)). However, after 120 s of HIFU exposure (Fig. 3b (x-xii)), there was a substantial improvement in the disruption of the well-organized biofilm structure. Minimal *E. faecalis* biofilm remained within the root canal, extending up to the apical part (Fig. 3b (xii)). Additionally, with 120 s of HIFU exposure, it appeared that the smear layers were removed, exposing the dentinal tubules, and creating a textured surface on the dentine, extending from the coronal to the apical part (Fig. 3b (x-xii)). Utilizing the Gutmann et al. (29) rating system, intergroup comparisons at the apical level revealed a statistically significant difference in smear layer removal effectiveness among the treatment groups ($p < 0.001$) (Fig. 3c). Specifically, 120 s of HIFU exposure demonstrated superior efficacy compared to 4% NaOCl in removing both the smear layer and *E. faecalis* biofilm.

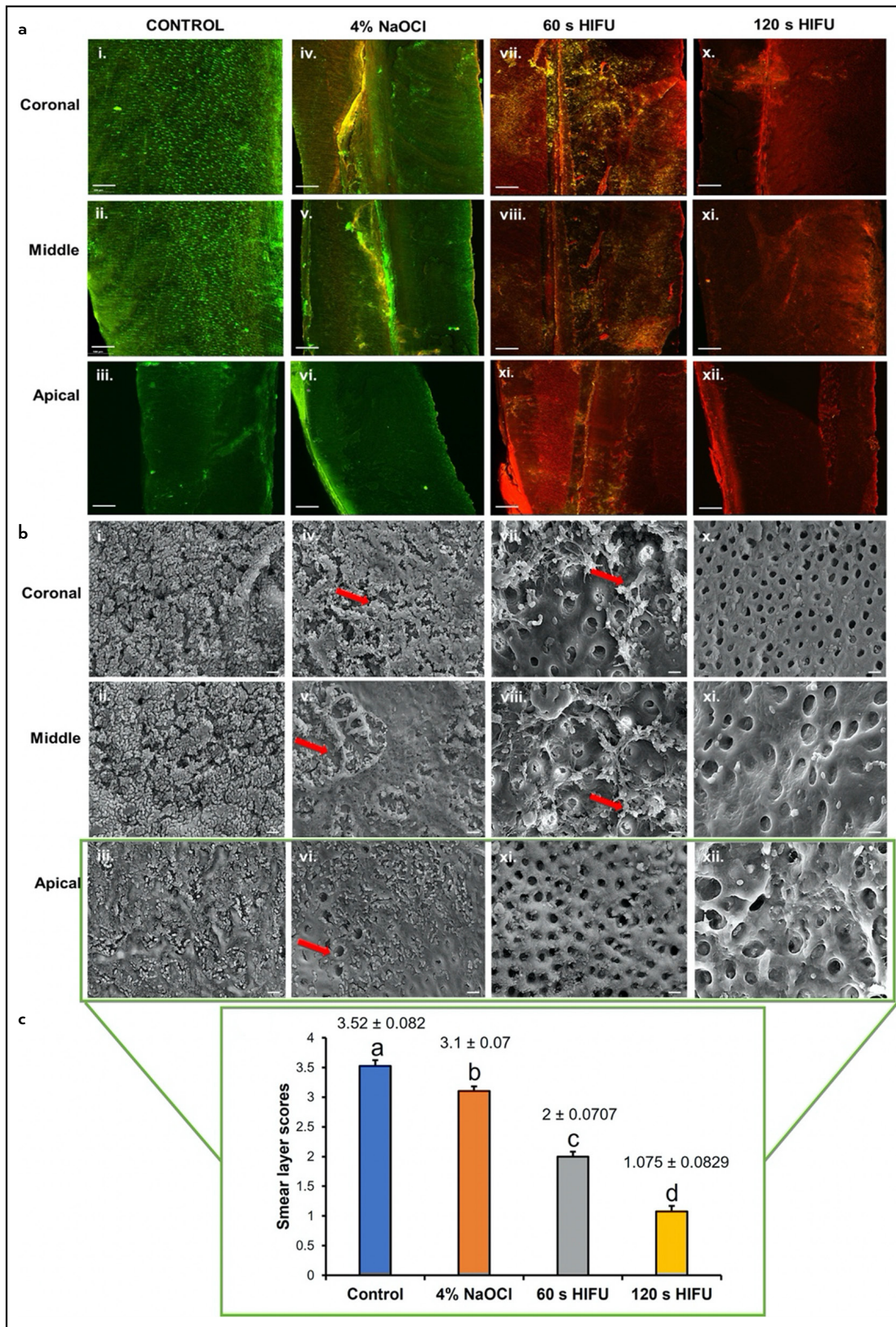


Figure 3. (a) Represent z-stacked confocal images (10X mag) of the root canal (coronal, middle, and apical) of the treatment groups (All bars represent 100 μm). (b) Represent the SEM images of the coronal, middle, and apical parts of the root canal after exposure to different treatment parameters. (Mag x7500) (All bars represent 2 μm). Red arrows- indicate disruption of the highly interconnected biofilm network. (c) The bar graph illustrates the intergroup comparison of remaining smear layer scores at the apical level among the treatment groups, as observed from SEM images (dissimilar letters indicate a significant difference at $p < 0.001$)

NaOCl: Sodium hypochlorite, HIFU: High-intensity focused ultrasound, SEM: Scanning electron microscope,

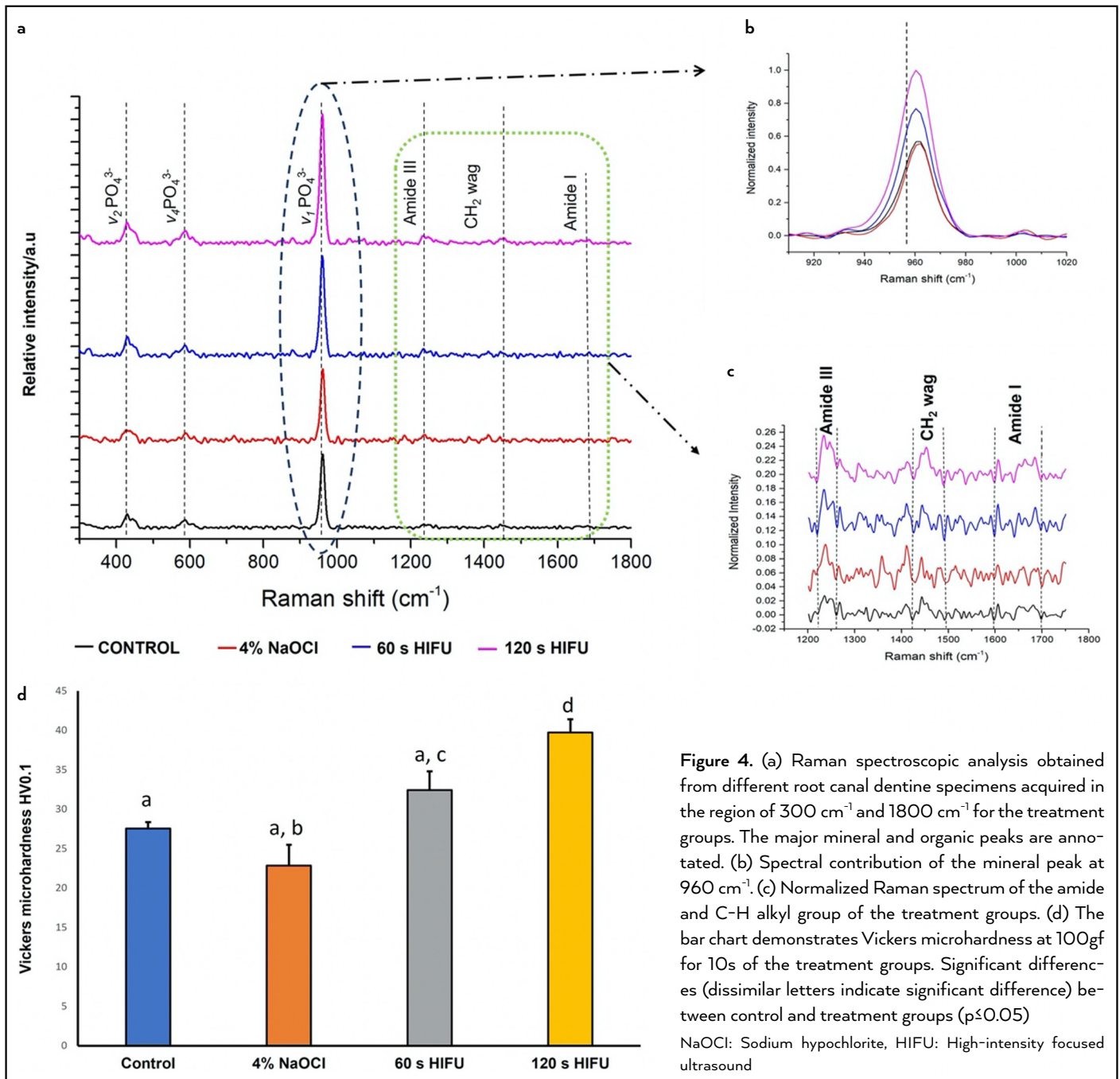


Figure 4. (a) Raman spectroscopic analysis obtained from different root canal dentine specimens acquired in the region of 300 cm⁻¹ and 1800 cm⁻¹ for the treatment groups. The major mineral and organic peaks are annotated. (b) Spectral contribution of the mineral peak at 960 cm⁻¹. (c) Normalized Raman spectrum of the amide and C-H alkyl group of the treatment groups. (d) The bar chart demonstrates Vickers microhardness at 100gf for 10s of the treatment groups. Significant differences (dissimilar letters indicate significant difference) between control and treatment groups ($p < 0.05$)

NaOCl: Sodium hypochlorite, HIFU: High-intensity focused ultrasound

Raman Analysis

The characteristic Raman spectra of root canal dentine of the treatment groups are displayed in Figure 4a. After treatment with HIFU, it was observed that the root canal dentine specimens exhibited an elevated amide/mineral intensity ratio. Notably, the most prominent band at 960 cm⁻¹ was associated with the symmetric stretching mode of $\nu_1\text{PO}_4^{3-}$, while bands at 429 cm⁻¹ and 588 cm⁻¹ corresponded to $\nu_2\text{PO}_4^{3-}$ and $\nu_4\text{PO}_4^{3-}$, at 1254 cm⁻¹ to Amide III, at 1442 cm⁻¹ to CH₂ wag, and the peak at 1683 cm⁻¹ to Amide I. The intensities at 960 cm⁻¹, 1254 cm⁻¹, 1442 cm⁻¹, and 1683 cm⁻¹ were more pronounced for the HIFU treatment groups (Fig. 4b, c).

Vickers Microhardness Testing

Mechanical properties of the root canal surface that underwent treatment were measured and expressed as mean ±

standard deviation, using Vickers microhardness (VH) (Fig. 4d). Among the treatment groups, the root canal surface treated with 4% NaOCl exhibited the lowest VH value, measuring 22.84 ± 2.64, in comparison to the other treatment groups. However, following 120 s of HIFU exposure, the VH value significantly increased to 39.71 ± 1.7, and this increase was statistically significant when compared to the other groups ($p < 0.05$). This observed rise in VH values for specimens exposed to HIFU could potentially be linked to the removal of the smear layer, as demonstrated in the SEM images (Fig. 3b (x-xii)).

HIFU Penetration/Distribution and Temperature Change Within RCS

The infiltration of ultrasound gel containing FITC into the RCS under varying HIFU exposure conditions is illustrated in Fig-

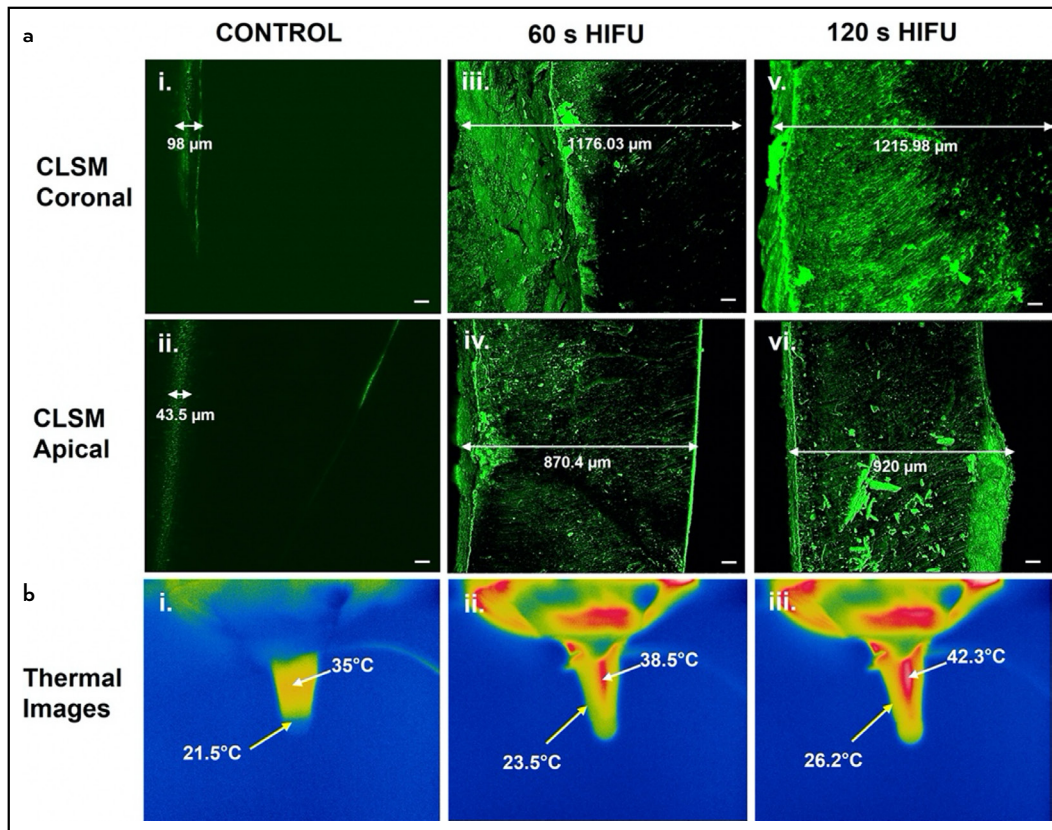


Figure 5. (a) Representative CLSM images (10X mag) showing the ability of HIFU waves to penetrate within the dentinal tubules and across the RCS (All bars represent 50 μm) (double-sided arrows display the penetration distance). (b) Thermal images of the root canal specimen demonstrating the heat distribution within the RCS during HIFU treatments. The white arrow represents the temperature change occurring within the RCS; the yellow arrow indicates the temperature change at the external surface of the root canal

HIFU: High-intensity focused ultrasound, CLSM: Confocal laser scanning microscopy, RCS: Root canal system

ure 5a. The CLSM images reveal that in the control group (Fig. 5a (i, ii)), the penetration of FITC-incorporated ultrasound gel is limited to approximately $\sim 98 \pm 15.8$ μm in the coronal part and about $\sim 43.5 \pm 6.5$ μm in the apical part of the RCS. However, when the specimens are exposed to HIFU (Fig. 5a (iii-vi)), there is a time-dependent increase in how far the gel can infiltrate both horizontally and vertically within the RCS. Simultaneously, thermal images of the root canal specimen were recorded to visualize the temperature change occurring within the system. Figure 5b iii shows that exposure to 120 s of HIFU resulted in a localized temperature increase ($\sim 42.3 \pm 1.5^\circ\text{C}$) within the RCS when compared to the control ($\sim 35 \pm 2^\circ\text{C}$) (Fig. 5b (i)). Importantly, the temperature at the external root surface remained below $26 \pm 1.25^\circ\text{C}$, ensuring the safety and integrity of surrounding structures.

DISCUSSION

This study investigated the effect of high-intensity focused ultrasound (HIFU) on the reduction of intracanal *E. faecalis* biofilm and evaluated its chemical and mechanical effects on the dentine surface for potential application in root canal treatment. *E. Faecalis* was the organism of choice, in this study, due to its association with various forms of periapical diseases (33). The physiological characteristics and structural nature of *E. Faecalis* biofilm, including its enhanced ability to invade dentinal tubules and adhere strongly to dentine collagen, provide augmented protec-

tion against antimicrobial agents (34, 35). Therefore, *E. faecalis* poses a therapeutic challenge to clinicians due to its propensity for acquiring and transferring antimicrobial drug resistance (36).

In this study, the anti-bacterial effectiveness of all treatments was evaluated by assessing two key parameters: metabolic activity, measured through MTT, and the ability to form new colonies (CFU). NaOCl is a potent disinfecting agent known for its anti-bacterial action against *E. faecalis* biofilm (26, 27). Despite its widespread use as a root canal irrigant, the optimal concentration of NaOCl in clinical endodontics remains controversial, with recommendations ranging from $<1\%$ to $>5\%$ (6, 37). In this study, a 4% NaOCl was used based on evidence indicating that concentrations above 5% can lead to significant degradation of the organic dentine matrix and severe caustic effects on apical tissues (38, 39). However, our findings indicate that treatments involving varying times of HIFU exposure, especially 120 s, demonstrated superior efficacy in biofilm removal compared to irrigation with 4% NaOCl, as evidenced by reduced metabolic activity and bacterial colony formation (Fig. 2 a, 2b).

Exposure to different treatments can render some cells non-viable, although they may exhibit limited respiration for a brief period (17). Hence, the CFU assay was performed concurrently with the MTT assay. Although NaOCl exhibited some anti-

bacterial activity compared to the control, it fell short of completely eradicating or disrupting the bacterial biofilm from the root canal wall and proved ineffective in penetrating dentinal tubules to eliminate the bacteria residing within. Conversely, the anti-bacterial effect observed following HIFU exposure is likely attributed to the generation of mechanical shock waves, which disrupt bacterial cell walls and lead to the formation of reactive oxygen species (ROS) such as $\text{OH}\cdot$, $\text{HO}_2\cdot$, $\text{O}\cdot$, and H_2O_2 . These ROS can cause damage to bacterial membranes, proteins, DNA, and RNA (40–42). Moreover, the creation of shock waves results in increased conversion of acoustic energy to heat, which propagates throughout the sample due to thermal diffusion (42). Elevated temperatures can weaken the bacterial cell envelope, rendering them more susceptible to cavitation effects (43).

The CLSM technique was further performed to investigate the spatial distribution of bacteria within the coronal, middle, and apical parts of the root canal. Additionally, SEM was utilized to examine the biofilm adherence and structure on the root canal surface. The CLSM and SEM images provided supporting evidence for the bacterial count reduction. These images revealed that the treatment methods involving HIFU with different exposure times exhibited improved penetration and detachment of biofilm when compared to NaOCl irrigation (Fig. 3a).

Following a 120 s treatment with HIFU, the root canal surface topography demonstrated an increased detachment of the densely interconnected bacterial structures within the canal. In contrast, while NaOCl managed to disrupt the biofilm organization, bacteria remained adhered to the root canal, resulting in alterations to the canal surface (Fig. 3b). This is significant because the persistence of microorganisms in the canal system can lead to root canal treatment failure. Consequently, it underscores the limited efficacy of irrigants alone in fully erad-

icating bacteria from the dentinal tubules (44). Contrarily, the findings from Vyas et al. (18) indicate that the advantage of utilizing HIFU, as opposed to other methods, primarily lies in the ability of acoustic waves' capacity to deeply penetrate dentinal tubules and disrupt biofilm structure, ultimately detaching bacteria from the surface. Furthermore, because bacteria have limited opportunity to adapt to sustained mechanical waves, HIFU treatment poses a lower risk of resistance development (45). Further, to better understand the penetration/distribution and temperature change of HIFU within the RCS, the root canal specimens were injected with ultrasound coupling gel containing the FITC stain and subjected to varying HIFU treatment times. The treated samples were then visualized using CLSM to assess the acoustic wave distribution pattern and the distance the waves can penetrate within the dentinal tubules.

Thermal imaging was also performed to monitor the generation of heat during the procedure, as observed by Canney et al. (42). The CLSM images demonstrate that HIFU exposure for 60 s and 120 s facilitated the penetration of the stained ultrasound gel deep within the dentinal tubules throughout the entire RCS, in contrast to the control (Fig. 5a). Studies have demonstrated the ability of chemical irrigants to penetrate deep into the dentinal tubules is generally restricted to around 160 μm (46, 47). However, this study has presented promising findings regarding the use of HIFU to detach or eliminate bacteria residing deep within the dentinal tubules, achieving a depth of approximately $\sim 1176 \pm 42 \mu\text{m}$. In addition, the thermal images reveal a noticeable increase in localized temperature and heat dissipation within the RCS during HIFU exposure, attaining a peak temperature of 42.3°C during 120 s of HIFU treatment. Moreover, the external root surface temperature remained below $26 \pm 1.25^\circ\text{C}$ at 120 s of HIFU exposure, which is within the tolerance threshold of the surrounding structures, thus preserving their structural integrity

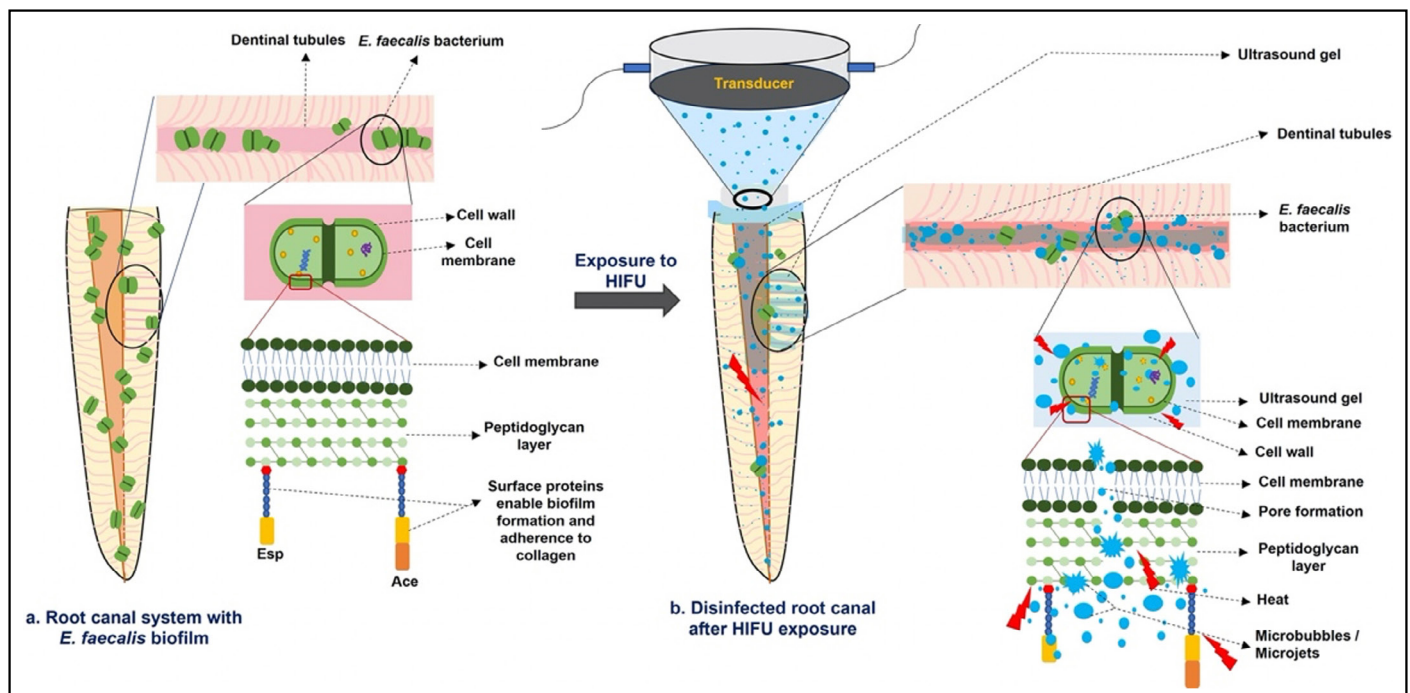


Figure 6. Diagram of the postulated anti-bacterial mechanism of HIFU against *E. faecalis* biofilm in root canal

HIFU: High-intensity focused ultrasound

(Fig. 5b) (48). These results suggest that the potential removal and destruction of bacteria from the RCS may be attributed to a combined effect of the elevated temperature and the propagation of acoustic waves occurring during HIFU exposure (Fig. 6).

Raman spectroscopy was performed as a quantitative method for assessing the chemical composition of dentine and provides valuable insights into the amide/mineral content. The results obtained through Raman spectroscopy revealed a decrease in the peak height and area of 960 cm^{-1} for the NaOCl group. In contrast, specimens exposed to HIFU exhibited the highest peak intensities in the phosphate band compared to the control. Amide bands present in the Raman spectrum are indicative of the stability of the collagen structure, attributed to hydrogen bonding between glycine and proline (49). The Amide I, Amide III, and CH_2 wagging peaks are clearly identifiable in the Raman spectra of both the control and HIFU-exposed groups, as shown in Figure 4c. However, these peaks showed a reduction in intensity in the NaOCl group. The decrease in the Amide I (1683 cm^{-1}) peak in the NaOCl group suggests potential damage or removal of the collagen fibril, and the lower intensity of CH_2 wag implies decreased concentrations of proteins, lipids, and carbohydrates (50). In contrast, the increased concentrations of Amide I, Amide III, CH_2 wag, and PO_4^{3-} suggest that treatment with HIFU could possibly reverse dentine deproteination.

Examining the surface microhardness provides indirect insights into mineral changes in dental hard tissues. The findings in this study, align well with the microscopic (Fig. 3c) and spectroscopic analysis (Fig. 4a-c). Notably, exposure to 120 s of HIFU resulted in a significant increase ($p < 0.05$) in surface hardness compared to the control group (Fig. 4d). This increase in surface hardness could potentially be attributed to the ability of HIFU to remove the smear layer (Fig. 3c), revealing the underlying dentine, and facilitating better penetration of the acoustic waves, as visualized by SEM images and CLSM. On the other hand, utilization of NaOCl solution for 1 min led to a decrease in the surface hardness values of the root canal, probably due to the dissolution of exposed organic components of the dentine. The changes in intensity ratios and altered surface hardness profile observed in the HIFU-treated groups suggest that HIFU exposure has the potential to not only destroy or detach bacteria but also to remove the smear layer and demineralized surfaces, thereby exposing the healthy dentine underneath, which contributes to better sealer penetration and enhanced root canal filling. Further investigations are warranted to gain a deeper understanding of how HIFU enhances microhardness and the relative intensity of demineralized root canal dentine substrates.

This study showed the promising anti-bacterial effect of HIFU exposure on *E. faecalis* biofilms and demonstrated acoustic wave penetration/distribution with the associated temperature change inside the RCS within the used exposure parameters and set-up. However, the results presented are obtained from a laboratory model, which is the main limitation of this study. More clinically relevant HIFU exposure set-up and parameter re-validation are required as a step forward toward the potential of translating this technology to clinical endodontics. Also, further investigation on a multi-species biofilm should be conducted.

CONCLUSION

In-vitro experiments utilizing HIFU with a frequency of 250 kHz and an output power of 20 W demonstrated significant anti-bacterial efficacy against *E. faecalis* biofilms. The efficacy of this treatment was found to be positively correlated with the duration of exposure, up to 120 s. Importantly, this anti-bacterial effect was achieved without causing detrimental changes to the amide and mineral content of root dentine or compromising its surface microhardness. These findings highlight HIFU as a promising minimally invasive technique for the effective removal of bacterial biofilms within the RCS, suggesting its potential as a valuable adjunct to conventional root canal disinfection methods.

Disclosures

Acknowledgments: The authors would like to acknowledge Minh Dien Tran, and Cheryl Fu for their assistance in sample preparation.

Ethics Committee Approval: The study was approved by the University of Western Australia Human Research Ethics Committee (no: #RE 2019/RA/4/20/5863, date: 17/06/2021).

Authorship Contributions: Concept – S.M.R., A.F.; Design – S.M.R., A.F.; Supervision – A.F.; Funding – S.M.R., A.F.; Materials – S.M.R.; Data collection and/or processing – S.M.R.; Data analysis and/or interpretation – S.M.R., B.S.; Writing – S.M.R.; Critical review – S.M.R., B.S., H.M.A.A., M.M.A.E., A.F.

Conflict of Interest: All authors declared no conflict of interest.

Use of AI for Writing Assistance: The authors declared that no artificial intelligence (AI)- assisted technologies were used in the production of this manuscript.

Financial Disclosure: The author acknowledges the University of Western Australia's support through a 'Scholarship for International Research Fees and University Postgraduate Award (UPA); and the funding support from the National Health and Medical Research Council (NHMRC) [1188401], and Australian Dental Research Foundation (ADRF) [0229-2022]. The authors acknowledge the facilities, scientific, and technical assistance of Microscopy Australia at the Centre for Microscopy, Characterisation & Analysis, The University of Western Australia, a facility funded by the University, State, and Commonwealth Governments.

Peer-review: Externally peer-reviewed.

REFERENCES

1. Siqueira JF Jr, Rocas IN. Present status and future directions: Microbiology of endodontic infections. *Int Endod J* 2022; 55(Suppl 3):512–30. [CrossRef]
2. Trope M, Debelian G. Microbial control: the first stage of root canal treatment. *Gen Dent* 2009; 57(6):580–8.
3. Perez AR, Ricucci D, Vieira GCS, Provenzano JC, Alves FRF, Marcelliano-Alves MF, et al. Cleaning, shaping, and disinfecting abilities of 2 instrument systems as evaluated by a correlative micro-computed tomographic and histobacteriologic approach. *J Endod* 2020; 46(6):846–57. [CrossRef]
4. Vera J, Siqueira JF Jr, Ricucci D, Loghin S, Fernandez N, Flores B, et al. One-versus two-visit endodontic treatment of teeth with apical periodontitis: a histobacteriologic study. *J Endod* 2012; 38(8):1040–52. [CrossRef]
5. Vieira AR, Siqueira JF, Ricucci D, Lopes WSP. Dentinal tubule infection as the cause of recurrent disease and late endodontic treatment failure: a case report. *J Endod* 2012; 38(2):250–4. [CrossRef]
6. Boutsoukis C, Arias-Moliz MT. Present status and future directions - irrigants and irrigation methods. *Int Endod J* 2022; 55(Suppl 3):588–612. [CrossRef]
7. Ordinola-Zapata R, Noblett WC, Perez-Ron A, Ye Z, Vera J. Present status and future directions of intracanal medicaments. *Int Endod J* 2022; 55(Suppl 3):613–36. [CrossRef]
8. Fimple JL, Fontana CR, Foschi F, Ruggiero K, Song X, Pagonis TC, et al. Photodynamic treatment of endodontic polymicrobial infection *in vitro*. *J Endod* 2008; 34(6):728–34. [CrossRef]

9. Golob BS, Olivi G, Vrabec M, El Feghali R, Parker S, Benedicenti S. Efficacy of photon-induced photoacoustic streaming in the reduction of *enterococcus faecalis* within the root canal: different settings and different sodium hypochlorite concentrations. *J Endod* 2017; 43(10):1730–5. [\[CrossRef\]](#)
10. Wong J, Manoilo D, Nasman P, Belibasakis GN, Neelakantan P. Microbiological aspects of root canal infections and disinfection strategies: an update review on the current knowledge and challenges. *Front Oral Health* 2021; 2:672887. [\[CrossRef\]](#)
11. Aslantas EE, Buzoglu HD, Altundasar E, Serper A. Effect of EDTA, sodium hypochlorite, and chlorhexidine gluconate with or without surface modifiers on dentin microhardness. *J Endod* 2014; 40(6):876–9. [\[CrossRef\]](#)
12. Li Q, Zhang Q, Zou X, Yue L. Evaluation of four final irrigation protocols for cleaning root canal walls. *Int J Oral Sci* 2020; 12(1):29. [\[CrossRef\]](#)
13. Harrison AJ, Chivatxaranukul P, Parashos P, Messer HH. The effect of ultrasonically activated irrigation on reduction of *Enterococcus faecalis* in experimentally infected root canals. *Int Endod J* 2010; 43(11):968–77. [\[CrossRef\]](#)
14. Vieira AR, Siqueira JF Jr, Ricucci D, Lopes WS. Dentinal tubule infection as the cause of recurrent disease and late endodontic treatment failure: a case report. *J Endod* 2012; 38(2):250–4. [\[CrossRef\]](#)
15. Nair PN, Henry S, Cano V, Vera J. Microbial status of apical root canal system of human mandibular first molars with primary apical periodontitis after "one-visit" endodontic treatment. *Oral Surg Oral Med Oral Pathol Oral Radiol Endod* 2005; 99(2):231–52. [\[CrossRef\]](#)
16. Iqbal K, Ohi SW, Khoo BC, Neo J, Fawzy AS. Effect of high-intensity focused ultrasound on *Enterococcus faecalis* planktonic suspensions and biofilms. *Ultrasound Med Biol* 2013; 39(5):825–33. [\[CrossRef\]](#)
17. Rajan SM, Shrestha B, Aati S, Kujan O, Tay A, Fawzy AS. Evaluation of antibacterial efficacy of high-intensity focused ultrasound versus photodynamic therapy against *enterococcus faecalis*-infected root canals. *Ultrasound Med Biol* 2023; 49(8):1875–81. [\[CrossRef\]](#)
18. Vyas N, Wang QX, Manmi KA, Sammons RL, Kuehne SA, Walmsley AD. How does ultrasonic cavitation remove dental bacterial biofilm? *Ultrasound Sonochem* 2020; 67:105112. [\[CrossRef\]](#)
19. Felver B, King DC, Lea SC, Price GJ, Damien Walmsley A. Cavitation occurrence around ultrasonic dental scalers. *Ultrasound Sonochem* 2009; 16(5):692–7. [\[CrossRef\]](#)
20. Pandur Z, Dular M, Kostanjsek R, Stopar D. Bacterial cell wall material properties determine *E. coli* resistance to sonolysis. *Ultrasound Sonochem* 2022; 83:105919. [\[CrossRef\]](#)
21. Zupanc M, Pandur Z, Stepisnik Perdih T, Stopar D, Petkovsek M, Dular M. Effects of cavitation on different microorganisms: the current understanding of the mechanisms taking place behind the phenomenon. A review and proposals for further research. *Ultrasound Sonochem* 2019; 57:147–65. [\[CrossRef\]](#)
22. Fawzy AS, Daood U, Matinlinna JP. Potential of high-intensity focused ultrasound in resin-dentine bonding. *Dent Mater* 2019; 35(7):979–89. [\[CrossRef\]](#)
23. Bruhl M, Urban K, Donnermeyer D, Schafer E, Burklein S. Tube technique with light-curing composite for removing fractured root canal instruments: influence of polymerization cycles and mechanical exposure. *J Endod* 2020; 46(3):425–30. [\[CrossRef\]](#)
24. Psimma Z, Boutsoukis C, Vasiliadis L, Kastrinakis E. A new method for real-time quantification of irrigant extrusion during root canal irrigation *ex vivo*. *Int Endod J* 2013; 46(7):619–31. [\[CrossRef\]](#)
25. Oncag O, Hosgor M, Hilmioglu S, Zekioglu O, Eronat C, Burhanoglu D. Comparison of antibacterial and toxic effects of various root canal irrigants. *Int Endod J* 2003; 36(6):423–32. [\[CrossRef\]](#)
26. Seet AN, Zilm PS, Gully NJ, Cathro PR. Qualitative comparison of sonic or laser energisation of 4% sodium hypochlorite on an *Enterococcus faecalis* biofilm grown *in vitro*. *Aust Endod J* 2012; 38(3):100–6. [\[CrossRef\]](#)
27. Siqueira JF Jr, Machado AG, Silveira RM, Lopes HP, de Uzeda M. Evaluation of the effectiveness of sodium hypochlorite used with three irrigation methods in the elimination of *Enterococcus faecalis* from the root canal, *in vitro*. *Int Endod J* 1997; 30(4):279–82. [\[CrossRef\]](#)
28. Ordinola-Zapata R, Bramante CM, Apreccio RM, Handsides R, Jaramillo DE. Biofilm removal by 6% sodium hypochlorite activated by different irrigation techniques. *Int Endod J* 2014; 47(7):659–66. [\[CrossRef\]](#)
29. Gutmann JL, Saunders WP, Nguyen L, Guo IY, Saunders EM. Ultrasonic root-end preparation. Part 1. SEM analysis. *Int Endod J* 1994; 27(6):318–24. [\[CrossRef\]](#)
30. Oliveira LD, Carvalho CA, Nunes W, Valera MC, Camargo CH, Jorge AO. Effects of chlorhexidine and sodium hypochlorite on the microhardness of root canal dentin. *Oral Surg Oral Med Oral Pathol Oral Radiol Endod* 2007; 104(4):e125–8. [\[CrossRef\]](#)
31. Budd JC, Gekelman D, White JM. Temperature rise of the post and on the root surface during ultrasonic post removal. *Int Endod J* 2005; 38(10):705–11. [\[CrossRef\]](#)
32. Lipski M, Debicki M, Drozdziak A. Effect of different water flows on root surface temperature during ultrasonic removal of posts. *Oral Surg Oral Med Oral Pathol Oral Radiol Endod* 2010; 110(3):395–400. [\[CrossRef\]](#)
33. Stuart CH, Schwartz SA, Beeson TJ, Owatz CB. *Enterococcus faecalis*: its role in root canal treatment failure and current concepts in retreatment. *J Endod* 2006; 32(2):93–8. [\[CrossRef\]](#)
34. Siqueira JF Jr, Rocas IN. Community as the unit of pathogenicity: an emerging concept as to the microbial pathogenesis of apical periodontitis. *Oral Surg Oral Med Oral Pathol Oral Radiol Endod* 2009; 107(6):870–8. [\[CrossRef\]](#)
35. Ran S, Wang J, Jiang W, Zhu C, Liang J. Assessment of dentinal tubule invasion capacity of *Enterococcus faecalis* under stress conditions *ex vivo*. *Int Endod J* 2015; 48(4):362–72. [\[CrossRef\]](#)
36. Krawczyk B, Wityk P, Galecka M, Michalik M. The many faces of enterococcus spp.-commensal, probiotic and opportunistic pathogen. *Microorganisms* 2021; 9(9):1900. [\[CrossRef\]](#)
37. Zehnder M. Root canal irrigants. *J Endod* 2006; 32(5):389–98. [\[CrossRef\]](#)
38. Jaiswal N, Sinha DJ, Singh UP, Singh K, Jandial UA, Goel S. Evaluation of antibacterial efficacy of Chitosan, Chlorhexidine, Propolis and Sodium hypochlorite on *Enterococcus faecalis* biofilm: an *in vitro* study. *J Clin Exp Dent* 2017; 9(9):e1066–74. [\[CrossRef\]](#)
39. Goncalves LS, Rodrigues RC, Andrade Junior CV, Soares RG, Vettore MV. The effect of sodium hypochlorite and chlorhexidine as irrigant solutions for root canal disinfection: a systematic review of clinical trials. *J Endod* 2016; 42(4):527–32. [\[CrossRef\]](#)
40. Vyas N, Manmi K, Wang Q, Jadhav AJ, Barigou M, Sammons RL, et al. Which parameters affect biofilm removal with acoustic cavitation? A review. *Ultrasound Med Biol* 2019; 45(5):1044–55. [\[CrossRef\]](#)
41. Brayman AA, MacConaghy BE, Wang YN, Chan KT, Monsky WL, McClenny AJ, et al. Inactivation of planktonic *Escherichia coli* by focused 2-MHz ultrasound. *Ultrasound Med Biol* 2017; 43(7):1476–85. [\[CrossRef\]](#)
42. Canney MS, Khokhlova VA, Bessonova OV, Bailey MR, Crum LA. Shock-induced heating and millisecond boiling in gels and tissue due to high intensity focused ultrasound. *Ultrasound Med Biol* 2010; 36(2):250–67. [\[CrossRef\]](#)
43. Li J, Suo Y, Liao X, Ahn J, Liu D, Chen S, et al. Analysis of *Staphylococcus aureus* cell viability, sublethal injury and death induced by synergistic combination of ultrasound and mild heat. *Ultrasound Sonochem* 2017; 39:101–10. [\[CrossRef\]](#)
44. Sundqvist G, Figdor D, Persson S, Sjogren U. Microbiologic analysis of teeth with failed endodontic treatment and the outcome of conservative re-treatment. *Oral Surg Oral Med Oral Pathol Oral Radiol Endod* 1998; 85(1):86–93. [\[CrossRef\]](#)
45. Vollmer AC, Kwakye S, Halpern M, Everbach EC. Bacterial stress responses to 1-megahertz pulsed ultrasound in the presence of microbubbles. *Appl Environ Microbiol* 1998; 64(10):3927–31. [\[CrossRef\]](#)
46. Berutti E, Marini R, Angeretti A. Penetration ability of different irrigants into dentinal tubules. *J Endod* 1997; 23(12):725–7. [\[CrossRef\]](#)
47. Giardino L, Pedulla E, Cavani F, Bisciotti F, Giannetti L, Checchi V, et al. Comparative evaluation of the penetration depth into dentinal tubules of three endodontic irrigants. *Materials (Basel)* 2021; 14(19):5853. [\[CrossRef\]](#)
48. Kwon SJ, Park YJ, Jun SH, Ahn JS, Lee IB, Cho BH, et al. Thermal irritation of teeth during dental treatment procedures. *Restor Dent Endod* 2013; 38(3):105–12. [\[CrossRef\]](#)
49. Daood U, Fawzy AS. Minimally invasive high-intensity focused ultrasound (HIFU) improves dentine remineralization with hydroxyapatite nanorods. *Dent Mater* 2020; 36(3):456–67. [\[CrossRef\]](#)
50. He Z, Chen L, Hu X, Shimada Y, Otsuki M, Tagami J, et al. Mechanical properties and molecular structure analysis of subsurface dentin after Er:YAG laser irradiation. *J Mech Behav Biomed Mater* 2017; 74:274–82. [\[CrossRef\]](#)